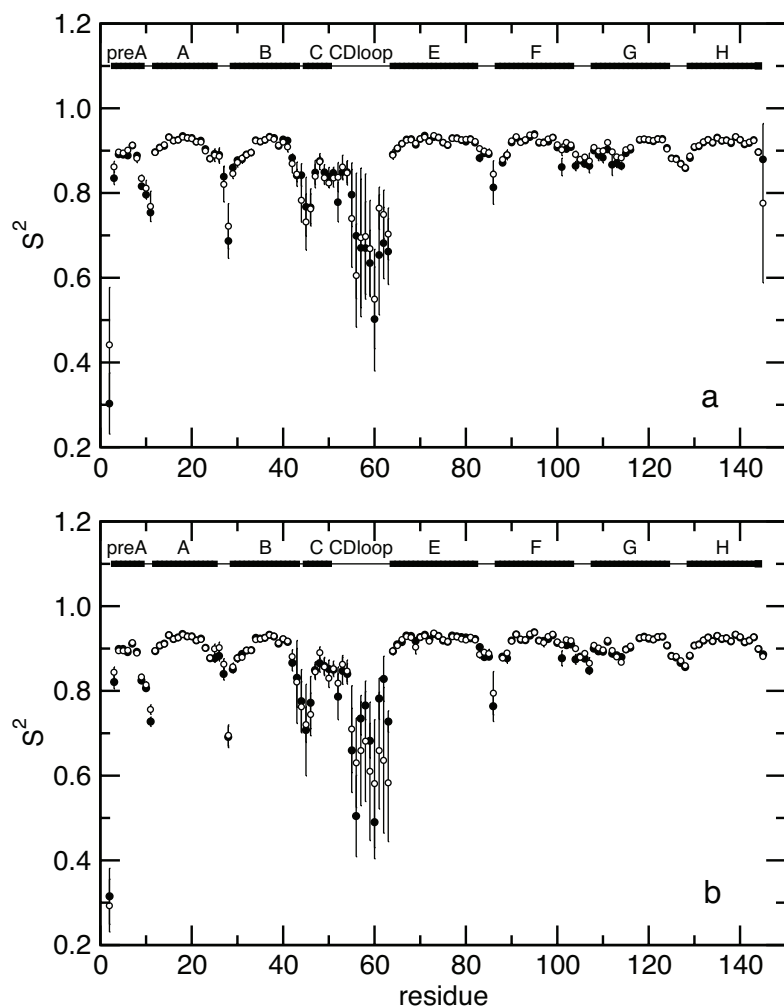


## Supporting Information

	CO-HbI	HbI	CO-F97Y HbI	F97Y HbI
a. Not assigned	2, 12, 56, 81, 130	2, 70, 71, 73-75, 77, 97, 99-103, 105, 106, 111-114	2, 12, 56, 81, 99, 117, 130	2, 12, 36, 42, 50, 51, 53, 56, 65, 69-77, 97-107, 113, 117, 130
b. No relaxation parameters due to severe spectral overlap	3, 5, 6, 8, 23, 27, 28, 37, 39, 42, 43, 57, 58, 61, 63, 70, 82, 86, 89, 93, 95, 100, 104, 107, 114, 118, 120, 129, 131, 133, 137	5, 12, 15, 17, 23, 24, 27, 28, 30, 36, 37, 42, 44, 53, 56, 58, 72, 91, 104, 107, 137	16, 21, 23, 27, 28, 29, 31, 39, 42, 43, 44, 49, 55, 57-60, 63, 69, 71, 72, 78, 83, 86, 89, 92-94, 97, 103, 104, 107, 114, 115, 118-120, 124, 131, 137	5, 10, 11, 16, 18, 19, 21, 23, 27, 29, 39, 48, 62, 63, 65, 66, 78, 80-82, 89, 93, 114, 119-121, 123, 127, 129, 136, 141
c. No relaxation parameters due to low S/N ratio	53, 103, 110, 115	33, 48, 50, 51, 54, 69, 73, 76, 79, 81, 82, 90, 93, 94, 102, 109, 115, 130, 141, 142, 143	53, 96, 101, 102, 142	14, 30, 37, 40, 47, 54, 57, 61, 63, 64, 79, 96, 112, 115, 122, 140, 142, 146

Table S1. Missing residues from the NMR relaxation studies of HbI and F97Y HbI in the free and bound states. a) Residues that could not be assigned due to overlap or lack of signal. b) Residues whose relaxation parameters could not be accurately determined because of severe spectral overlap. c) Residues whose relaxation parameters could not be accurately determined due to the errors resulting from low signal intensities in one or more of the relaxation experiments.



**Figure S1.** Backbone NH order parameters ( $S^2$ ) of HbI and F97Y HbI calculated from the MD simulations. Order parameters,  $S^2$  are shown as a function of the residue number for WT HbI (a) and F97Y HbI (b).  $S^2$  values calculated for CO-bound HbI are shown as closed circles,  $S^2$  values for unliganded HbI are shown as open circles. Secondary structural elements are shown at the top of each plot. Solid bars represent  $\alpha$ -helices and lines represent loops.

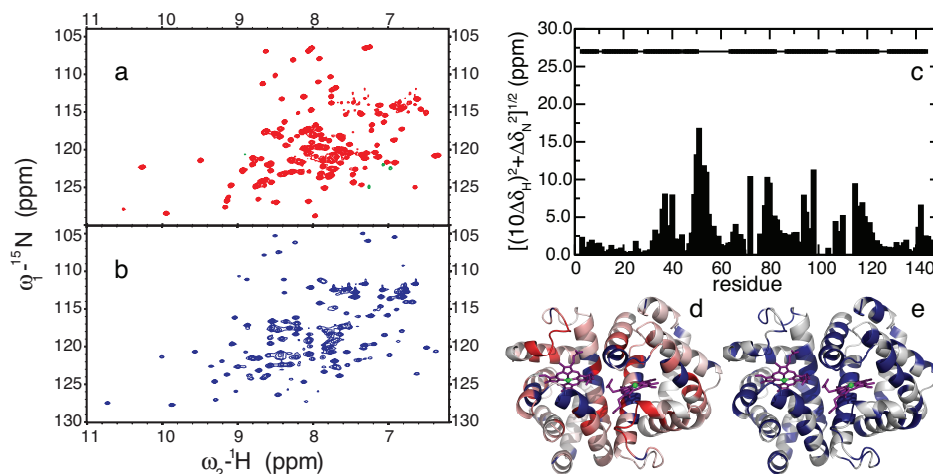


**Figure S2.**  $^1\text{H}$ ,  $^{15}\text{N}$  TROSY correlation spectrum is shown for uniformly labeled  $^2\text{H}/^{15}\text{N}$  HbI in CO-bound (a) and free (b) states. Chemical shift changes,  $[(10\Delta\delta_{\text{H}})^2 + \Delta\delta_{\text{N}}^2]^{1/2}$ , in HbI upon binding of CO are shown as a function of the residue number in (c).  $\Delta\delta_{\text{N}}$  and  $\Delta\delta_{\text{H}}$  are the chemical shift changes for  $^{15}\text{N}$  and  $^1\text{H}$  resonances in ppm, respectively. The values of  $[(10\Delta\delta_{\text{H}})^2 + \Delta\delta_{\text{N}}^2]^{1/2}$  are mapped onto the structure of the HbI monomer (d). The color scale goes from white (0 ppm) to red (17 ppm). Unassigned residues are shown in blue. The residues that could not be assigned (Table S1, row a) or residues excluded from the model-free analysis (Table S1, row b and c) are shown on the structure of the HbI monomer in blue (e). The structural representations were drawn using PyMOL<sup>1</sup>.

1. DeLano, W. L. (2002) *The PyMOL molecular graphics system*. DeLano Scientific, San Carlos, CA, USA.

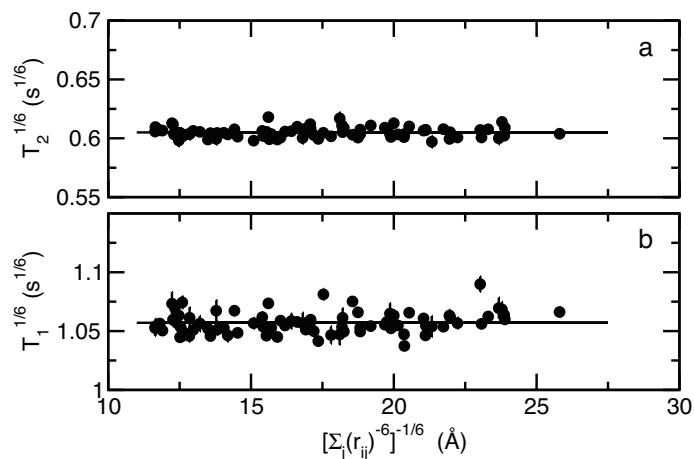


**Figure S3.** Plot of the longitudinal and transverse relaxation times,  $T_1$  and  $T_2$ , respectively, of all the residues used in the model-free analysis as a function of the distance from the paramagnetic  $\text{Fe}^{2+}$  ions.  $r_{ij}$  is the distance between an amide  $^{15}\text{N}$  atom,  $i$ , from one of the two  $\text{Fe}^{2+}$  ions,  $j$ . Because Hbl contains two  $\text{Fe}^{2+}$  ions, two  $^{15}\text{N}$ -Fe distances have to be considered for each amide group<sup>2</sup>. The relaxation times of all the residues used in the model-free analysis are independent from the distance to the  $\text{Fe}^{2+}$  ions indicating that the paramagnetic contribution to the relaxation rates is negligible. The solid line is the linear fit with slope of zero.

2. Bertini, I., Luchinat, C., and Piccioli, M. (2001) Paramagnetic probes in metalloproteins. *Methods Enzymol.* 339, 314-340.

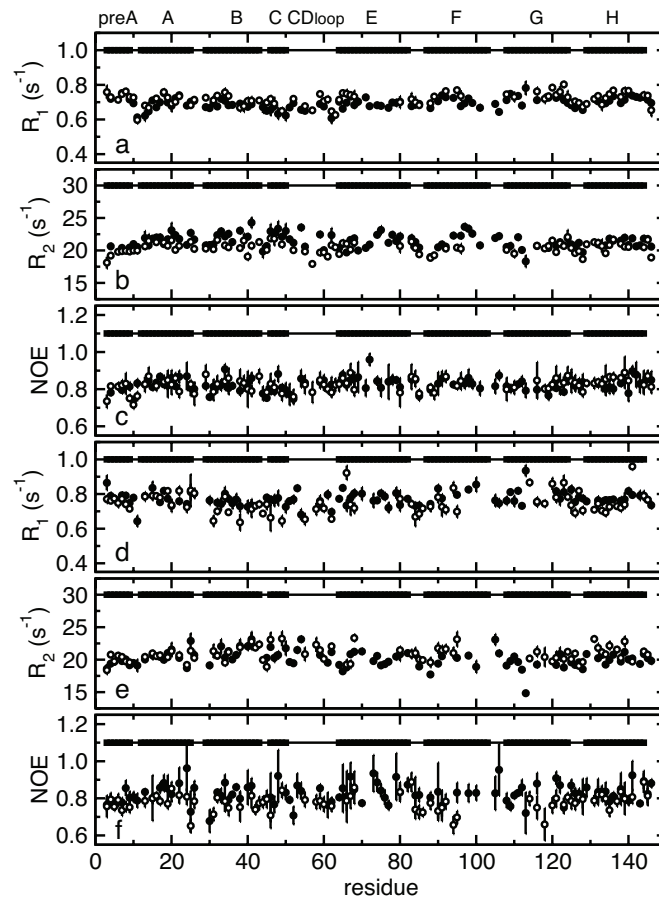


**Figure S4.** NMR relaxation rates of WT and F97Y HbI.  $^{15}\text{N}$  longitudinal,  $R_1$ , and transverse,  $R_2$ , relaxation rate constants, and  $\{^1\text{H}\}$ - $^{15}\text{N}$  nuclear Overhauser enhancement (NOE) measured for WT HbI (a, b, c) and F97Y HbI (d, e, f) in both the liganded (closed circle) and unliganded (open circles) states at 14.1 T and 298 K. The secondary structural elements are depicted at the top of each panel.

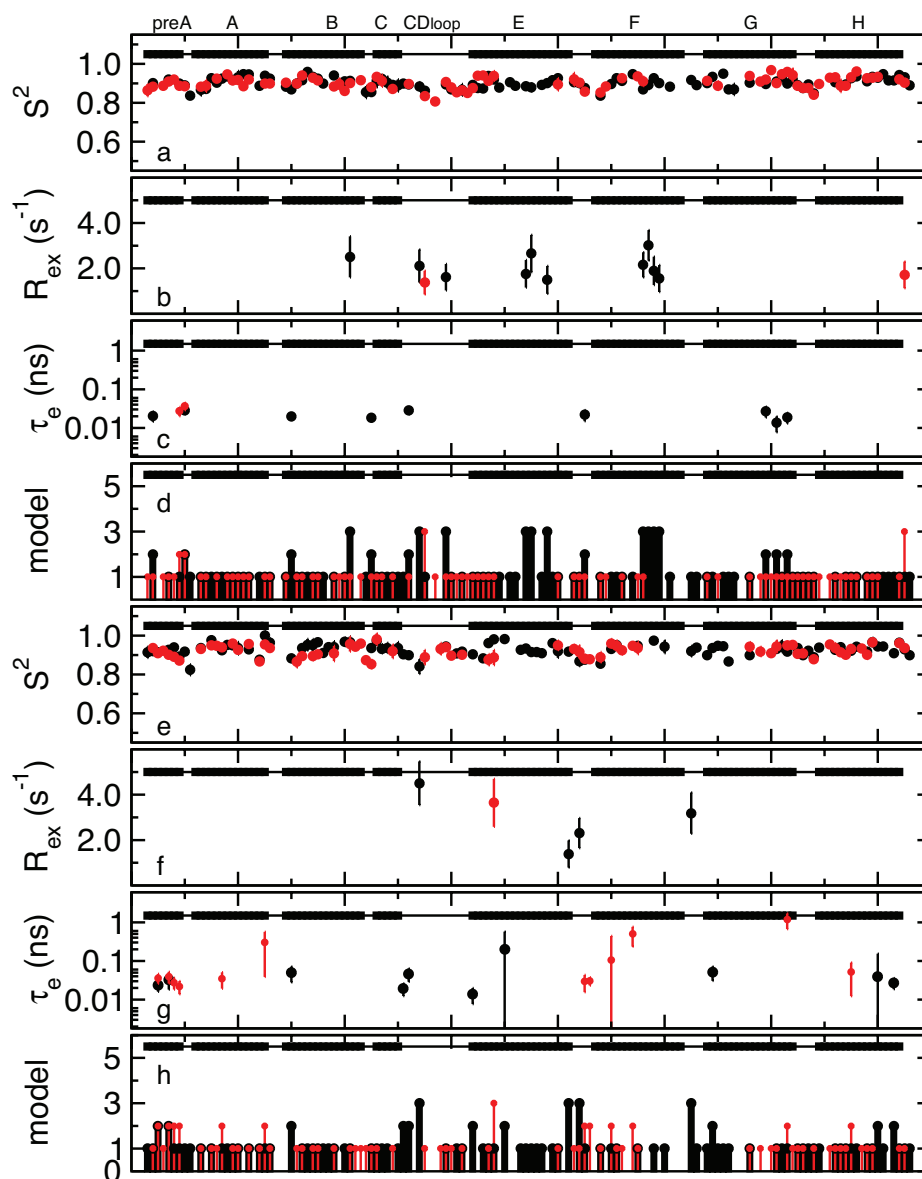


**Figure S5.** Internal dynamics of WT and F97Y HbI at 298 K. Model-free parameters describing amplitudes and time scales of motion on the ps – ns time scale are plotted for the free (red) and CO-bound (black) states of WT HbI (a, b, c, d) and F97Y HbI (e, f, g, h).  $S^2$  is the generalized order parameter, which defines the amplitude of the motion,  $\tau_e$  is an effective internal correlation time,  $R_{ex}$  is the chemical exchange contribution to  $R_2$  and model is motional model used in the relaxation data analysis. The secondary structural elements are depicted at the top of each panel.

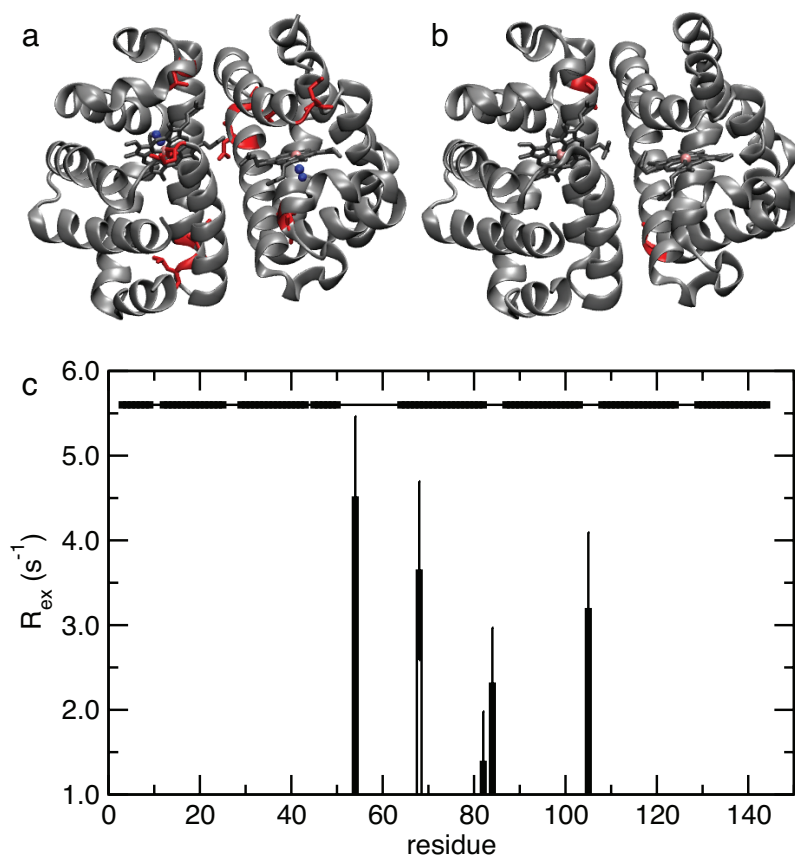


**Figure S6.** Chemical exchange contribution determined from the Lipari and Szabo model free analysis of the <sup>15</sup>N spin relaxation measurements parameters of F97-HbI. Residues with non-zero chemical exchange contributions,  $R_{ex}$ , determined from <sup>15</sup>N spin relaxation data, are mapped in red on the structure of the protein for CO-bound F97 HbI (a), and unliganded F97 HbI (b).  $R_{ex}$  is shown as a function of protein sequence with closed bars and open bars for CO-bound F97 HbI and unliganded F97 HbI, respectively (c). Secondary structural elements are shown at the top of the plot. Solid bars represent  $\alpha$ -helices and lines represent loops.